Achieving Solidification and Redispersion of Semiconducting Polymer Dots by Layered Double Hydroxide Incorporation

Xiao-Jie Liu, Wei Wang, Yo-Hong Chen, Joey Andrew A. Valinton, Yang-Hsiang Chan and Chun-Hu Chen**

Department of Chemistry, National Sun Yat-sen University, 70 Lien Hai Road, Kaohsiung, Taiwan 80424.

* E-mail: yhchan@mail.nsysu.edu.tw (YH Chan), chunhu.chen@mail.nsysu.edu.tw (CH Chen)

ABSTRACT: Solidification and aqueous redispersion of fluorophores are characteristically challenging due to aggregation quenching and random shifts of emission. Carbon-based polymer dots (PDs) have recently shown superior photoluminescent performance to conventional dyes and inorganic quantum dots (QDs), but suffer from significant fluorescence quenching and irreversible aqueous dispersion after solidification, which limits their applications in practical biomedicine and optical devices. In this work, we have compared three strategies by utilizing layered double hydroxide (LDH) to effectively solidify PDs as robust and redispersible composites with well-preserved high brightness against wide pH (pH = 4 to 12) and strong ionic strength conditions, more stable than the pristine PDs. The resulting PD-LDH nanocomposites also show *in vitro*/*in vivo* bio-imaging ability with low cytotoxicity and improved photostability. In addition, these composites exhibit high thermal stability at 150 ºC for at least 96 h. The composites produced by onr-step physical mixing approach (~ 10 min) of LDH and PDs (p-PLDH) exhibited comparable PL performance as compared to the conventional multi-step composites (m-PLDH) which require tremendous efforts (at least 7 days) to be prepared. Structural studies further revealed that the de-shaping behaviors of PDs and inter-flake sandwich assembly of LDH contributed to the robust fluorescence properties. Owing to the simple synthesis, durable photostability, high aqueous redispersion, and multicolor emissions (ranging from blue to near-infrared) of these PD-LDH nanocomposites, we believe that they are promising candidates for advanced bio-related technologies and optoelectronics.

KEYWORDS: layered double hydroxides, Polymer dots, bioimaging, solidification, photoluminescence, sandwich assembly

1. INTRODUCTION

Photoluminescent (PL) stable materials are highly desired for emission devices, biological imaging, and specific labeling.[1-4] However their solidification and aqueous redispersion without sacrificing PL properties are difficult to achieve due to aggregation quenching and unpredictable shifts of emission colors. Optical device miniaturization with concentrated brightness relies on the success of fluorophore solidification, while aqueous redispersion capability governs probing stability and diversity in biological imaging. Great efforts have been made to address these issues for high photostability, long-term storage, and convenient device engineering. For example, solidification of carbon dots (CDs) has been demonstrated by poly(vinyl alcohol) to generate soft grating films with bright emission; but the shift of emission wavelength, relatively low thermal stability (<400 K), and non-redispersibility remain unsolved.[5] Silane-mediated solidification on quantum dots (QDs)[6] and CDs[7] have been widely carried out by surface passivation to realize aggregation-free condensation. Their improved emission properties are accomplished; yet high material stability is required due to the harsh reaction conditions and complicated procedures adopted in the synthesis. In fact, reversible solidification and aqueous re-dispersion are characteristic issues in diverse light emitting materials (e.g. CDs, QDs, molecular dyes, polymer dots, etc.) for specific applications.[2, 5, 8-9]

Recently, semiconducting polymer dots (PDs) have attracted significant attention due to their superior brightness, quantum yields, absorptivity, radiative rates, and photostability as compared to conventional small organic dyes and inorganic QDs.[10-16] These carbon-based PDs have been approved to be non-cytotoxic, and more functionalization-capable than inorganic QDs, thus emerging as a new class of, photoluminescent[17-20] and photoacoustic[21-23] probes for biomedical

applications[24-25]. Nevertheless, similar to the issues above, solidification of PDs suffers from non-reversible aggregation (huge size increase after redispersion), reduced PL efficiency, and loss of bioconjugation capability. Thus PDs might need to be prepared freshly for immediate use because their PL efficiency might not remain unchanged for very long if no appropriate storage conditions (e.g., low temperature, minimal exposure to light) were adopted. This could greatly limit their potential of pre-synthesizing the ready-to-use PDs colloidal products for clinical and industrial usage. Chiu's group has recently developed a lyophilization process for long-term storage of PD bioconjugates; but the method requires the PDs to be constantly stored at -80 ºC.[26] Usually once PDs are dried out from aqueous solutions into the solid-state form, it is very difficult to gain re-dispersed aqueous PDs colloids again by simply adding water into the condensed PD powders.

Layered double hydroxides (LDH) are versatile layered materials with general formula of $[M^{II}_{1-x}M^{III}_{x}(OH^{-})_2]^{x+}[(A^{n-})_{x/n}\cdot yH_2O]^{x-}$ (M=metals and A=intercalated anions). Different PL materials,[27-31] including fluorescent dyes[8], biomolecules[32-33], quantum dots[9, 34-35], metal nanoclusters,[36] metal complexes[37], and room temperature phosphorescent (RTP) materials[38] were already been incorporated into LDH and exhibited sustained PL properties. Compared to other protective materials, LDH with adjustable sizes, low cytotoxicity, and weak fluorescent interference is advantageous to realize PL-reserved solidification. However, conventional LDH hybridization commonly involves exfoliation[36-37], which needs complicated procedures, harsh conditions like high basicity, high temperature conditions and long operation time. Alternative methods such as .co-precipitation[38-40], and hydrothermal[41] has also been developed. To simplify that into one-pot reaction, harsh conditions of high basicity and reaction temperatures should be addressed.

Herein, we have developed three various solidification methods to well preserve the fluorescence of PDs via incorporation with LDH (PD-LDH). All of the solidified, redispersible PD-LDH nanocomposites exhibited robust photostability (remained almost unchanged for at least 96 h) under various pH conditions (pH=4 to 12) and strong ionic-strength environments. In particular, the physical mixing synthesis (p-PLDH) with facile (as short as ~10 min) and single-step procedure at room temperatures represents the most efficient solidification process, rather than cryogenic and harsh preparation for days. The LDH nanoflakes manage to quickly sandwich PDs closely associated with their dimensional mismatch and soft nature of PDs, providing the practical synthetic designs capable of large scale and easy preparation of exfoliation-free, highly bright and stable PL nanocomposites. We further applied these PD-LDH nanocomposites for in vitro/in vivo bio-imaging to demonstrate their biological applications.

2. EXPERIMENTAL SECTION

2.1. Synthesis of LDH and PDs

The synthesis of nanosized LDH with diameters around 100 nm, an aqueous solution (90 mL) of $Mg(NO_3)_2 \cdot 6H_2O$ (2 M) and $Al(NO_3)_3 \cdot 9H_2O$ (1 M) was added into 300 mL of NaOH solution (0.6 M), followed by refluxing at 100ºC for 24 h.[29] The white precipitate was then centrifuged (8000 rpm) and washed by D.I. water for several times. The products were dried at 60ºC to obtain pristine LDH. The LDH [Mg]/[Al] ratio of 2.89 was determined using ICP-MS giving the formula of $[Mg^{II}_{0.74}Al^{III}_{0.26}(OH)_2]^{0.26+}[(NO_3)^-_{0.26} \cdot nH_2O]^{0.26-}$. For the synthesis of PDs, we added 200 μL of semiconducting polymer solution (1 mg/mL in THF) and 20 μL of PS-PEG-COOH (2 mg/mL in THF), where PS = polystyrene and PEG = poly(ethylene glycol), into 5 mL of THF. The solution

was mixed well and then quickly injected into 10 mL of water under vigorous sonication. After that, THF was removed at 96 ºC under nitrogen atmosphere to obtain PD solution.[12]

2.2. Synthesis of multiple-step PD-LDH (m-PLDH)

In a typical preparation of m-PLDH, the pristine LDH undergone ion-exchange, exfoliation, and recombination with negatively charged PDs. Ion exchange was conducted by adding 0.5 g LDH powder in a 500 mL aqueous solution of 2M NaCl and 3.3 mM HCl.[34,42-46] The mixture was stirred under N_2 for 3 days, followed by centrifuge, washing and drying procedures. The resultant (0.3 g) was added into 300 mL of formamide, and the mixture was stirred under N_2 for another 3 days.[47-48] The supernatant after centrifugation at 2000 rpm was collected for another centrifugation at 14,000 rpm. (5 min). The dried sediment (5 mg) as exfoliated LDH was dispersed into 1 mL of PDs solution (absorbance at 450 nm is 0.44) and then stirred in the dark for 3 h. The above procedures were all operated at room temperature. The mixture was then washed and dried.

2.3. Synthesis of single-step PD-LDH (s-PLDH)

A mixture of $Mg(NO_3)_2 \cdot 6H_2O$ (2 M, 3 mL) and $Al(NO_3)_3 \cdot 9H_2O$ (1 M, 3 mL) was added with 4 mL of NaOH (0.6 M) and then 6 mL of PD solution rapidly in a Teflon autoclave liner.[29] The resultant was then hydrothermally treated at 100 ºC for 8 hours. The product was washed, dried, and denoted as s-PLDH. For fluorescence measurement, the powder of 8.7 mg was dispersed into 1 mL water for further dilution.

2.4. Synthesis of physically mixed PD-LDH (p-PLDH)

The pristine LDH (5 mg) was mixed with 1 mL PD and stirred until homogeneously suspended for around 3 min. The mixture was washed by water and centrifuged at 14,000 rpm for 5 min.

2.5. Synthesis of PLDH-polyvinyl alcohol (PVA) film

For the PLDH-PVA film preparation, addition of 1 mL of PLDH suspension into 2 mL of PVA solution (20 wt %). was conducted. Here we used 20 % (w/w) PVA solution because of the modest solubility of PVA (Mw: 89,000-98,000) in 70 °C hot water and the appropriate mechanical properties as bendable films. After the gentle stirring to homogeneously mixed, the solution was transferred to culture plates and dried under the ambient conditions.

2.6. Materials and characterization

All chemicals were used directly without further purification. $Mg(NO_3)_2 \cdot 6H_2O$ and $Al(NO_3)_3 \cdot 9H_2O$ were purchased from Acros, and NaOH was purchased from Shimakyu. Synthesis of PDs with different emission wavelength was recorded in the literature.[12, 49] The PDs with yellow and red fluorescence are [poly(fluorene-alt-benzothiadiazole)] (PF-BT) and [poly[(9,9-dioctylfluorene)-co-2,1,3-benzothiadiazole-co-4,7-di(thiophen-2-yl)-2,1,3-benzo-thiadiazole] (PF-BT-DBT), respectively. The material morphology and crystallinity were determined by field-emission scanning electron microscopy (FEGSEM, JEOL-6330), X-ray diffraction (XRD, BRUKER D2 Phaser), and transmission electron microscopy (JEOL JEM-2100). The fluorescence spectra were acquired with Hitachi F-7000 (excitation wavelength = 450 nm). The emission behavior of PDs and the three PLDH composites were studied by adding 1 mL of dispersed PD or PLDH into 4 mL of water or buffer solution for the fluorescence intensity measurement, thermal stability experiments, and quantum yield measurements. The buffer solutions include 0.01 M and 0.1 M PBS with pH values of 4, 7, and 12 adjusted by HCl or NaOH. The thermal stability experiment was conducted by dropping 500 μL of PD and PLDH solution on 1 × 1 cm^2 of commercial PET films. After drying at 60ºC for 24 hours, the films were placed in an oven at 150 ℃ for certain time. Quantum yields were acquired by direct method with fluorescence spectra (Hitachi F-7000) coupled with an integrating sphere. In addition, the zeta potentials of the pristine

LDH, bare PDs, and p-PLDH were measured by a Zetasizer Nano system to be +54 mV, -34 mV and +47 mV, respectively. The reaction yields of m/s/p-PLDH are estimated by comparing the PL intensity of the colloidal PDs for PLDH preparation and the PL of the supernatant after PD solidification. Typically, the yields of all PLDH samples were in the range of 98-99%.

2.7. Bioimaging procedures

The transgenic zebrafish, Tg(kdrl:eGFP)la116 expressing eGFP in the endothelial cells, were kept at 28 °C and bred under standard conditions with approval from National Sun Yat-sen University Animal Care Committee. For angiography imaging, 37 nL PD (125 nM) in 20 mM HEPES buffer was injected into the sinus venosus of the anaesthetized zebrafish embryos three-day post fertilization (dpf) with 5% (v/v) tricaine. After 20 min recovery, the injected embryos were immobilized in 1.5% low melting point agarose (Sigma), and then imaged immediately by use of a fluorescence confocal microscope (Zeiss LSM 700).

The cervical cancer cell line HeLa was ordered from Food Industry Research and Development Institute (Taiwan). Primary cultured HeLa cells were grown in Dulbecco's Modified Eagle Medium (cat. no. 11885, Life Technologies) supplemented with 10% Fetal Bovine Serum and 1% penicillin-streptomycin solution (5000 units/mL penicillin G, 50 μg/mL streptomycin sulfate in 0.85% NaCl) at 37 °C with 5% CO_2 humidified atmosphere. The cells were pre-cultured in a T-25 flask and allowed to grow for 3-4 days prior to experiments until ca. 85% confluence was reached. To suspend cells, the adherent cancer cells were quickly rinsed with media and then incubated in 0.8 mL trypsin-ethylenediaminetetraacetic acid (EDTA) solution (0.25 w/v % trypsin, 0.25 g/L EDTA) at 37°C for 3 min. The cell suspension solution was then centrifuged at 1000 rpm for 5 min to precipitate the cells to the bottom of the tube. After taking out the upper media, the cells

were rinsed and re-suspended in 5 mL of culture media. Approximately tens of thousands of cells were split onto a glass-bottomed culture dish and allowed to grow for 12 h before PD tagging. For endocytosis, 100 μL of PLDH solutions was added into the flask containing cells and then incubated for 2h. Prior to fluorescence imaging, the cells were rinsed with PBS buffer to remove any non-specifically bound PLDH on the cell surface.

3. RESULTS AND DISCUSSION

3.1. Synthesis of PD-LDH nanocomposites

Functionalization of carboxyl (-COOH) groups by blending PS-PEG-COOH on the surface of PD is critical to ensure their stable dispersion in water and capable for further surface modification.[12] In addition, the negative charges on the surface of PD can also be attributed to the polymer oxidation in the nano-precipitation process by which PD was prepared.[50] After the proton dissociation of carboxyl groups in pH=7 water, the PD with negatively charged surfaces (i.e. zeta potential of -34 mV) can disperse well due to the electrostatic repulsion among nanoparticles. However, a more acidic condition (pH<5) would substantially inhibit the dissociation the carboxyl groups, and thus PD tend to aggregate immediately, leading to fluorescence fluctuation or even PL quenching. This issue could be more severe in pristine PD solidification.

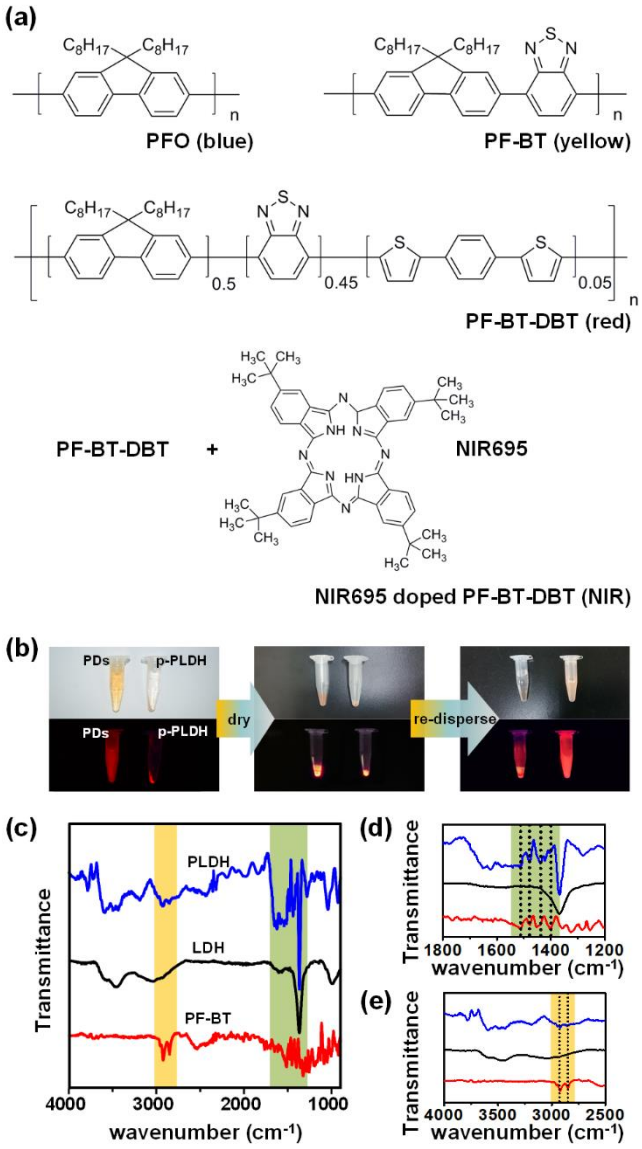

Figure 1. (a) Chemical structures of semiconducting polymers with abbreviation and emission colors. (b) Photographs of PF-BT-DBT PD and PF-BT-DBT p-PLDH after centrifugation at 14,000 rpm (left images), subsequently dried to remove water (middle images), and finally re-dispersed in water (right images). All the top photos are acquired under ambient light and the bottom ones are under 365 nm UV lamp. (c) The FTIR spectra of the PF-BT PD, pristine LDH, and PF-BT p-PLDH. The magnified spectra corresponding to the green and orange regions in (c) are shown in (d) and (e), respectively.

Various LDH comprised of different di- and trivalent metal ions (M^{2+}/M^{3+}) have been reported.[45-46, 51-52] Here we chose Mg/Al-LDH as our protecting material for PD because they have been demonstrated to exhibit high biocompatibility and no quenching effect towards fluorescent dyes.[29, 52-54] Besides, the surface charge of Mg/Al-LDH is positive and can combine well with the negatively charged PDs via the driving force of electrostatic interactions In terms of PD, we selected PD with four different emission colors (blue: PFO, yellow: PF-BT, red: PF-BT-DBT, and near-infrared: NIR695-doped PF-BT-DBT as shown in Figure 1a)[49] to examine the performance of PD-LDH hybrids. It is worth mentioning that yellow (PF-BT) and red (PF-BT-DBT) PD have already been extensively used for biological and sensing applications owing to their relatively high stability. Therefore, we took PF-BT and PF-BT-DBT as examples for our following initial assessments.

We compared three solidification strategies for the preparation of PD-LDH nanocomposites which are shown in Scheme 1. These strategies include: (i) multi-step, (ii) single-step, and (iii) physical-mixing methods. For multi-step approach, the synthesized LDH went through the conventional ion-exchange and exfoliation first, and then assembled with PDs to form PD-LDH nanocomposites (see Experimental Section for details). The hybrids formed by use of multi-step procedures are denoted as m-PLDH. Although these complicated syntheses have been widely adopted for molecular dye and quantum dot systems,[34] the overall processes are relatively inefficient and need at least one week to obtain the final products. To simplify the tedious synthetic procedures, we conducted the single-step strategy in which PDs were combined directly with metal precursors of LDH under hydrothermal treatments at 100 $^{\circ}$C. During the reaction, the cations of

Mg and Al might be attracted adjacent to the negatively charged PDs, and then sandwiched PDs directly to form PD-LDH nanocomposites (denoted as s-PLDH).

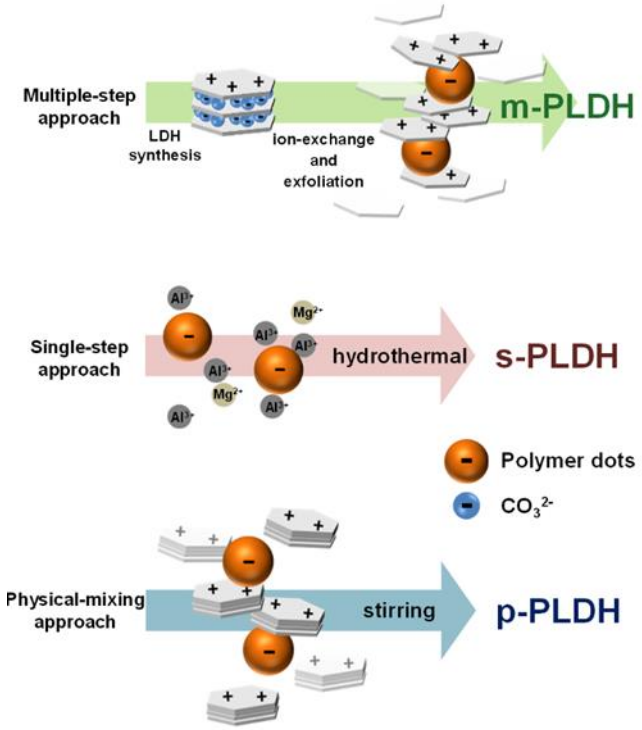

Scheme 1. Schematic illustration of the three approaches for the synthesis of PD-LDH nanocomposites.

It has been reported that physical incorporation of unexfoliated LDH into polymer matrix can enhance the polymer thermal stability and mechanical properties.[55-56] Therefore, we performed physical mixing approach by directly blending PDs with unexfoliated LDH to produce PD-LDH hybrids (denoted as p-PLDH). As compared to the synthesis of s-PLDH and m-PLDH composites, p-PLDH composites are much easier to be prepared.

3.2. PD solidification in PLDH

The solidification and redispersion performance of s-PLDH, m-PLDH, and p-PLDH nanocomposites were evaluated. In the case of PF-BT-DBT as p-PLDH, for example, complete precipitation was observed after centrifugation (left panel in Figure 1b). The supernatant, however, is essentially clear, colorless, and non-fluorescent under UV without any white powder suspension while the pellet is highly-colored and fluorescent under UV light, indicating a high degree of PD encapsulation within LDH. On the contrary, pure PDs were still suspended after centrifugation. We subsequently dried out the centrifuged p-PLDH and pure PDs under vacuum (middle panel of Figure 1b) to obtain their solidified products. The PL data show negligible emission change before and after the dry out step (Figure S1). We then redispersed the solidified p-PLDH and PDs by adding water under vigorous sonication in which p-PLDH composites achieved redispersion. These results have demonstrated that LDH could successfully solidify PDs and at the same time preserve their optical properties for further redispersion.

To verify the successful PD solidification with LDH, we conducted FTIR experiments as shown in Figure 1c-e in which the signature peaks were highlighted with orange and green stripes. The characteristic peaks of PDs at 2850 and 2920 cm^{-1} (the orange region) can be attributed to symmetric and asymmetric stretching mode of C-H bond in alkyl groups, while signals at 1390-1520 cm^{-1} (the green region) are assigned to vibrational features of conjugated polymer chain.[56-59] These signals could be observed in the PLDH but were absent in the pristine LDH, confirming the successful PD solidification with LDH.

3.3. Assembly studies of PLDH

It is important to understand the structural configurations of the solidification to correlate the preserved PL and high photostability. Figure S3a shows the XRD results of s/p/m- PLDH samples and pristine LDH. All these composites reveal similar characteristics with the intrinsic LDH, suggesting the identical interlayer spacing as pristine LDH. The absence of peaks with greater d-spacing than d_{003} in LDH indicates no intercalation occurred among the synthesized PLDH samples, including m-PLDH. Thus, LDH might hybridize PDs by sandwiching rather than interlayer intercalation, similar to the layer-by-layer assembly reported by Wei group.[55] In addition, we examined one of m-PLDH intermediates, Cl^- ion-exchanged LDH, showing the increased d-spacing of (003) by 0.19 Å (Fig. S3b).[34, 45] These results indicate the success of ion exchange, but LDH intercalation with PDs is not favored by following conventional ion-exchange, exfoliation, and recombination procedures. Therefore, the organic/inorganic interfacial behaviors and material natures of PD/LDH are quite different from that of all inorganic composite systems.[9, 34] On the other hand, the synthesized PLDH showing the same XRD patterns to LDH is reasonable, since no synthetic effort of ion-exchange or exfoliation is involved.

To visually monitor the PD/LDH interface, TEM and SEM characterization was carried out. The pristine Mg-Al LDH, prepared by reflux and hydrothermal methods, shows a characteristic hexagonal shape with the major size distribution around 80-100 nm, which is appropriate for *in vitro* cellular labelling and *in vivo* bio-imaging (Figure 2a and S4). As shown in Figure 2b, bare PD appeared to be spherical particle shapes with diameters of 20-30 nm, in the same order of magnitude as LDH. All the three PLDH nanocomposites showed the particle size distributions (105.31 ± 28.48 nm for m-PLDH; 91.93 ± 18.99 nm for s-PLDH; 94.63 ± 19.58 nm for p-PLDH) and morphologies similar to the pristine LDH (Figure 2c-e). However, the significant overlapping among PLDH flakes makes the clear identification of PDs to be difficult. Therefore, the location

of PDs and their interfaces with LDH were indistinguishable. The SEM images could not provide the indication of PDs adsorbed on the LDH surfaces (Figure S5).

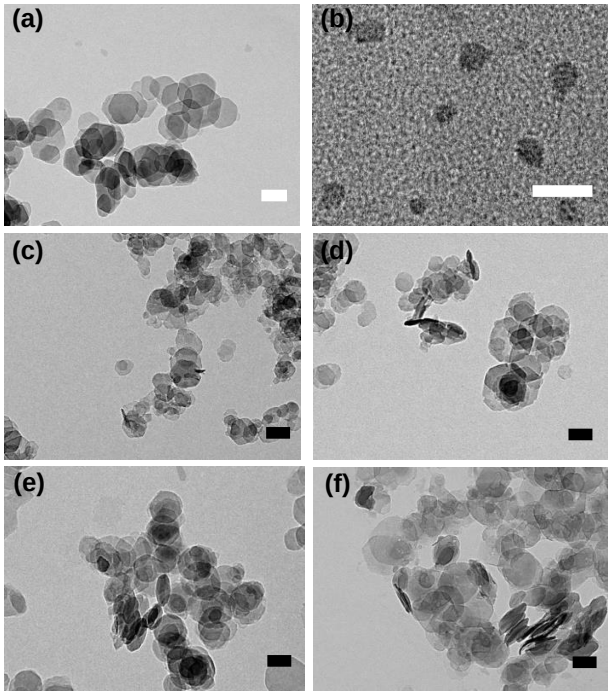

Figure 2. TEM images of (a) pristine LDH, (b) PD, (c) s-PLDH, (d) p-PLDH, (e) m-PLDH, and (f) m-PLDH with double amount of PD. The scale bar is 50 nm for (b) and 100 nm for the rest of images.

To identify the location of PDs and the hybridization interfaces, we further doubled the solidification quantity of PDs during the preparation of m-PLDH (Figure 2f), but, the PDs were still not distinguishable from the LDH flakes. Alternatively, TEM characterization particularly focusing on the vertically standing m-PLDH flakes was carried out. The appearance of vertical m-PLDH (Figure 3a) did not seem to encapsulate small spherical PDs between two LDH flakes. Interestingly, we found there exhibited many stacks of oval-like flakes (labelled by white dashed

line in Figure 3a). Besides, a shrinking behavior with the appreciable decrease of volume after the irradiation of focused electron beam could be observed (Figure 3b). Similar phenomenon was also observed in p-PLDH as shown in Figure 3c-d. Because of the robust property of LDH that it would not undergo deformation under electron beam irradiation, this shrinkage among the LDH flakes are more likely to be ascribed to the PD degradation. This phenomenon suggests that PDs should be sandwiched by and/or adsorbed on the LDH flakes. Besides, the non-spherical morphologies of PLDH (e.g. oval-like assemblies) suggests a deshaping mechanism of PDs after LDH sandwiching. Unlike rigid inorganic quantum dots, the carbon-based PDs are essentially soft enough to tolerate high degrees of morphological deshaping.

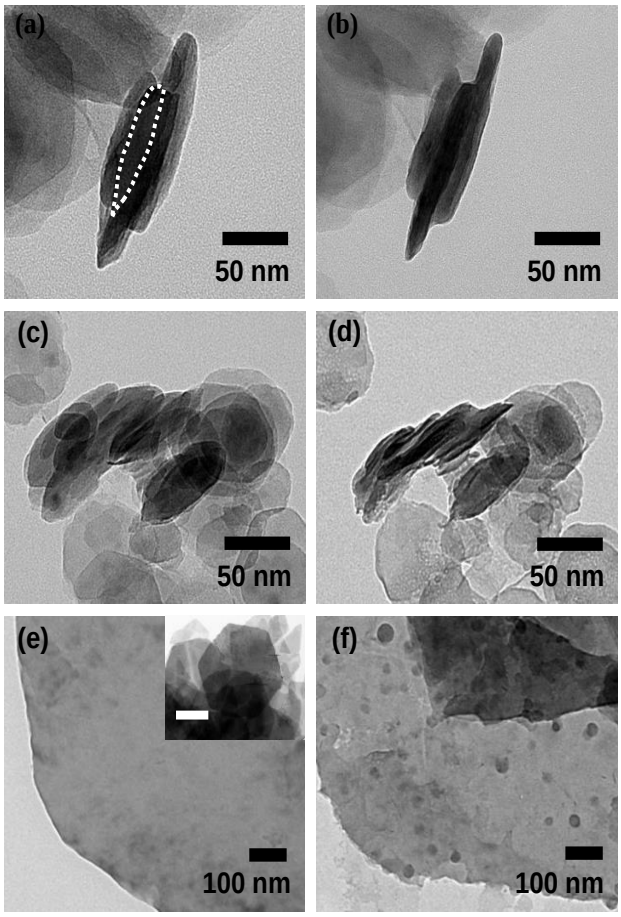

Figure 3. TEM images of m-PLDH composites before (a) and after (b) focused electron-beam irradiation. (c) and (d) are p-PLDH composites before and after focused electron-beam irradiation, respectively. (e) Bulky LDH with diameters of 2 μm before PD hybridization. The scale bar in the inset corresponds to 1 μm. (f) Bulky LDH after multi-step hybridization with PDs.

To confirm the deshaping behavior of hybridized PDs, we prepared wider LDH flakes (creating a drastic size difference from PD) with a diameter of ~2 μm[60] in order to provide sufficient surface areas for PD solidification with one individual LDH flake (Figure 3e). From TEM characterization, we could clearly observe the location of PDs with enlarged size distributions ranging from 40 to 70 nm (Figure 3f), showing the experimental support of the morphological deshaping. Furthermore, the deshaping effect of PDs after hybridization may explain the emission broadening

of PLDH (e.g. Figure 2). It has also been reported that the imperfect intercalation of soft biopolymer into LDH could occur after hybridization and further solidification. Based on the above experimental results, it is suggested that PDs are sandwiched by LDH flakes after the solidification. Due to the comparable sizes between individual LDH and deshaped PDs, the sandwich interaction (single LDH only carrying 1-2 PDs) isolates individual PDs from bulky aggregation to obtain robust fluorophore against harsh pH and strong ionic strength conditions even after solidification.

Although the full structural understanding of PLDH composites is still unclear at this stage, the experimental data strongly support that most PDs should be sandwiched among LDH flakes, regardless of which synthetic method in this study was employed. The PD, therefore, has a small possibility to be adsorbed on the exposed surfaces of LDH which affects fluorescence intensity of PD after incorporation. Similar sandwich incorporation of quantum dot with unexfoliated LDH for light emitting applications has been reported.[55] The unfavored PD intercalation in LDH galleries is presumably due to the drastic dimensional gap between thickness of exfoliated single LDH nanosheet (less than 1 nm) and the diameters of PDs (20-30 m). According to Gu et al,[61] the structure assembly of the relatively small LDH nanoflakes (tens of nanometers) and large volume cores (e.g. sub-micron scales of Fe_3O_4) [62] can lead to core/shell-like structures and varied orientations of the small objects (LDH nanoflakes), rather than LDH intercalation. The dimensional mismatches between PDs and the LDH composites are comparable to that model. Despite the absence of PD/LDH intercalation, their hierarchical assembly can be a novel pioneer of superstructured fluorophores. After all, among these PLDH nanocomposites, p-PLDH appeared to have the simplest and most efficient synthesis for achieving PD solidification and redispersion.

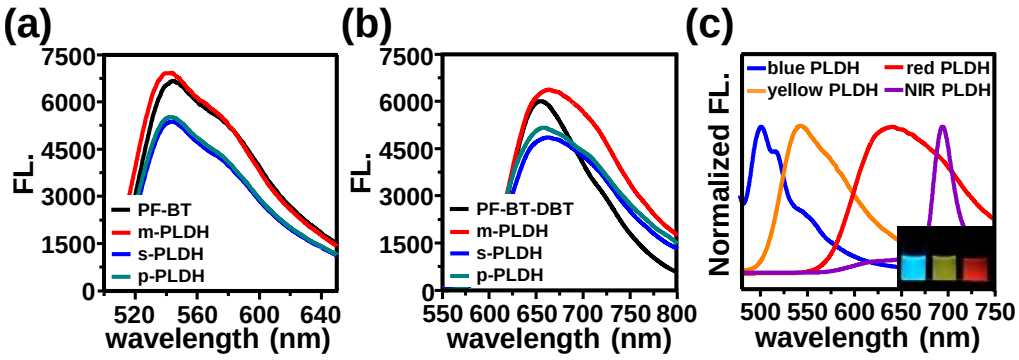

Figure 4. The fluorescent comparison of (a) yellow PDs (PFBT) and (b) red PDs (PFBT-DBT) with the corresponding PLDH composites. (c) m-PLDH of different emission wavelength from 500 to 700 nm. The inset picture is the fluorescent photographs of blue, yellow, and red m-PLDH samples corresponding to the spectra in (c).

3.4. Fluorescence study

Figure 4 shows the fluorescence spectra of PF-BT and PF-BT-DBT PD and their corresponding PLDH nanocomposites prepared by three different solidification approaches. All of the PF-BT and PF-BT-DBT m/s/p-PLDH nanocomposites showed the characteristic emission peaks identical to the pristine PDs with slight peak broadening (Figure 4a-b), suggesting possible minor morphology changes of PDs after solidification.[63] We found that m-PLDH showed the highest fluorescence intensity as compared to s-PLDH and p-PLDH. In the synthesis of s-PLDH, the highly basic preparation involving strong base of NaOH under pressurized hydrothermal treatments at 100°C was attributed to the reduced emission of PDs. For p-PLDH hybrids, their emission intensity was slightly higher than s-PLDH yet lower than m-PLDH. p-PLDH, represents the most facile and time-effective approach to obtain emissive PLDH whose microstructural assembly and fluorescence are comparable to other PLDH synthesized through other means in this study; hence, we selected physical mixing as the primary synthetic method to exhibit other properties in this work.

To evaluate the FL quenching of PDs after solidification, we measured the quantum yields (QY) of solidified/redispersed PD in water after the dried-out treatment as presented in Figure 1b. The results show a quenched QY of 11%, while the re-dispersed m/s/p-PLDH give a QY range (see Table S1) close to pristine PDs (~30%)[12]. The large difference in QY between unprotected PD attempting redispersion and PLDH means that quenching due to aggregation of PD is minimized in PLDH. Furthermore, the emission of all the PLDH composites remains stable for aging (at least 48 h, also see Figure 5) and repeated cycles of solidification/redispersion treatments. These data clearly verify that LDH incorporation is an effective strategy to well preserve FL of PDs as bright fluorophores against solidification and redispersion without the need of cryogenic conditions in aqueous solutions, which is practically valuable for manufacture process of various optical devices. We further measured the fluorescence lifetime by a time-correlated single-photon counting module system. As shown in Figure S8, we found that the fluorescence lifetime of bare PF-BT-DBT PDs was 4.33 ns and slightly decreased to 3.63 ns after LDH hybridization. This is probably due to some metal ions in LDH that might increases the non-radiative decay rate constant of PD. In addition, we further show that the incorporation of different types of PDs with diverse fluorescent colors (blue, yellow, red, and near infrared in LDH can also be synthesized (Figure 4c), suggesting that the LDH solidification method used in this study is universal for polymer-based nanoparticles.

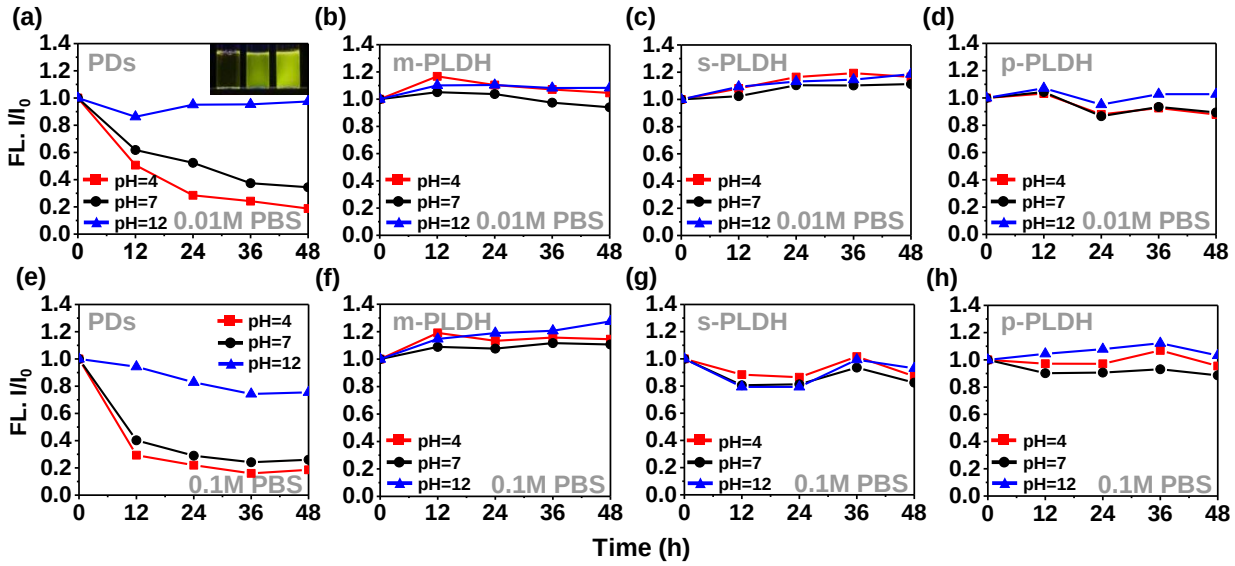

Figure 5. Photostability of the pristine PDs and the PLDH composites under varied pH and ionic strength conditions. The data of (a) to (d) are acquired in 0.01 M PBS with the pH values of 4, 7, and 12; those of (e) to (h) are recorded by increasing PBS concentration to 0.1 M. The inset in (a) shows PF-BT PDs suspended in 0.01 M PBS at pH=4, 7, 12 (from left to right respectively) for 48 h under UV lamp excitation.

3.5. Fluorescent stability

Since many biological systems are not completely neutral and may contain varied concentrations of different ions, the photostability of all the solidified PLDH was examined against harsh aqueous conditions with pH values of 4, 7, and 12. The data has confirmed that the as-prepared LDH can be stable under pH=4 at least for one month (See Figure S2). The effects of pH on PDs and PLDH were systematically investigated by fluorescence measurement based on the intensity ratios I/I_0. As shown in Figure 3a, in the case of 0.01 M phosphate-buffered saline (PBS), the fluorescence intensity of PDs decreases rapidly at pH=4 in which less than 50% and 20% of PL remained after 12-h and 48-h exposure, respectively. This quenching behavior is ascribed to the nanoparticle

aggregations after the COOH protonation on the PD surfaces. Such quenching can also be easily observed through the naked eye under UV excitation (Figure 5a inset). The fluorescence intensity of PDs in neutral buffer solution was gradually quenched due to the large ionic strength. In the pH=12 condition, PDs showed a decreased fluorescence immediately, followed by a recovery or even a slightly increased emission intensity (*vide infra* Figure 5a). This phenomenon might be associated with the increase of ionic strength and dissociation of COOH groups. In contrast, the fluorescence intensities of m/s/p-PLDH were very stable under different pH conditions (Figure 4b-d). This indicates that the presence of LDH can greatly preserve the optical stability of PD because LDH may isolate the hybridized PDs from protonation and sever aggregation. At this stage, no performance difference can be observed among the products by the three solidification methods.

It is known that FL stability of PDs depend on the quantity of surface charges, particularly under conditions of high ionic strength.[16, 64] The photostability of bare PDs with PLDH was evaluated and compared in increasing ionic strength. As shown in Figure 4e-h, we examined the optical stability of PDs and PLDH in 0.1 M PBS (ten times more concentrated than widely adopted 0.01 M environment).[65] The emission intensities of bare PDs were severely affected in 0.1 M PBS, and even more serious in acidic conditions. Despite the higher ionic strength conditions, all the PLDH composites still displayed high photostability at different pH conditions. According to Jin et. al.,[64] the successful improvement of PD colloidal stability through surface polyelectrolyte coating has be achieved under 1x PBS. Our results show the even greater photostability of PDs against 10x PBS conditions are now feasible via PD-LDH solidification. Because of the high photostability, good fluorescence quantum yield, and facile synthetic procedures of p-PLDH, we selected p-PLDH for further bio-imaging applications and thermal endurance assessment.

3.5. Bioimaging

The toxicity of bare PDs have been previously tested by several different groups, suggesting the minimal cytotoxicity of PDs.[16, 49, 66] We here examined the toxicity of PF-BT-DBT p-PLDH by using MTT assay and found out that PF-BT-DBT p-PLDH has minimal cytotoxic effect on cells while maintaining photostability under a 408 nm laser, as seen in Figure 6a-b. This is probably due to the protection of LDH against photo-oxidation , thus allowing a longer operation time of fluorescent probing than pristine PDs *in vivo*. We also labelled the cells with PF-BT-DBT p-PLDH via endocytosis. Figure 6c-e shows the confocal microscopy images of HeLa cells after the endocytosis of p-PLDH, clearly revealing that p-PLDH nanocomposites could be labelled onto cells for advanced biological applications.

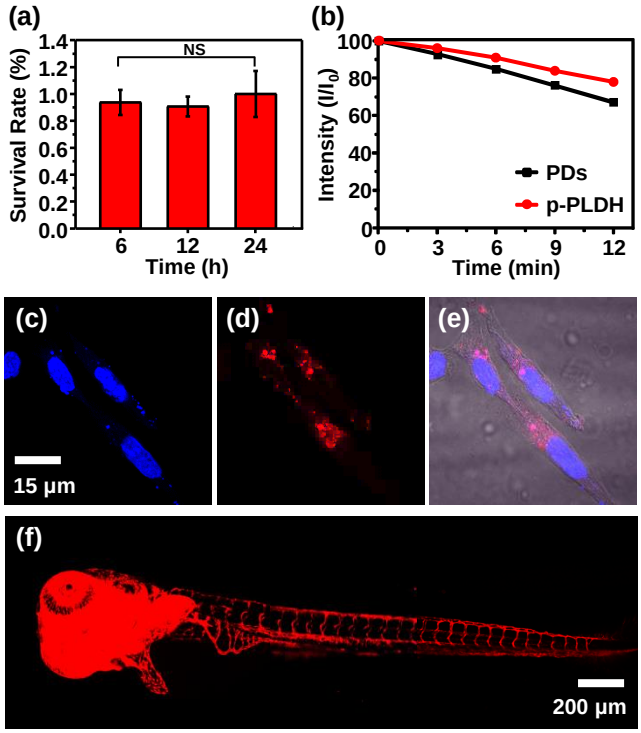

Figure 6. (a) Cytotoxicity tests of PF-BT-DBT p-PLDH with 98 % survival rate after 24 h. Values are expressed as the means ± SD (error bars). Statistical significance was determined by a two-tailed t-test. (b) Photostability of PDs (Abs = 1) and p-PLDH under continuous irradiation of 408 nm laser. Confocal fluorescence images of HeLa cells labeled with p-PLDH. The blue fluorescence

in (c) was from nuclear counterstain Hoechst 34580 and the red fluorescence in (d) was from p-PLDH. The overlay image of panel c, d, and bright-filed image was shown in (e). (f) Zebrafish microangiography by injection of p-PLDH with the scale bar of 500 mm.

For *in vivo* imaging, we first added PD solutions with different concentrations into zebrafish embryos. We then injected p-PLDH into the sinus venosus of the zebrafish larva and the red fluorescence from p-PLDH could be clearly observed immediately in the lumen of the vessels (Figure 4f). These results together with the cellular labelling demonstrated that p-PLDH exhibits excellent biocompatibility and optical stability which are ideal for biological imaging.

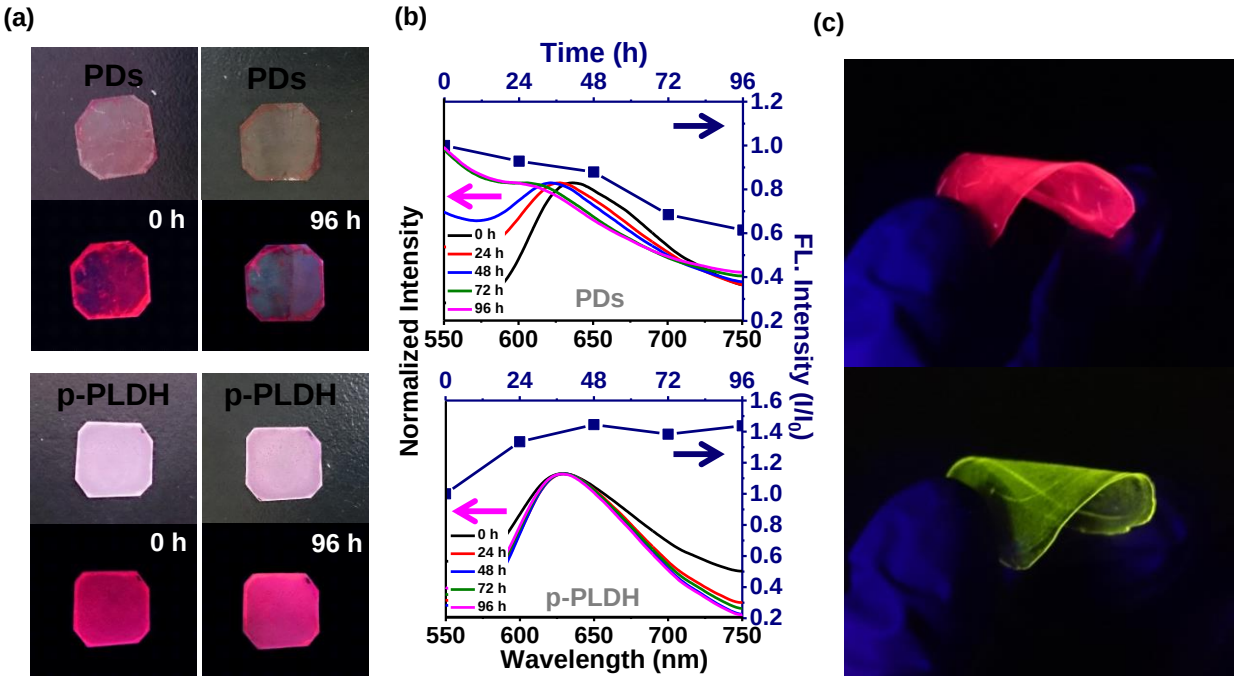

Figure 7. Thermal endurance tests of the bare PD and p-PLDH films. (a) Photograph comparison of PD and PLDH films on PET films after baking at 150ºC for 96 h; the lower images were acquired under 365 nm UV illumination. (b) Normalized fluorescence spectra and the

corresponding intensity plots of the PD (the upper one) and p-PLDH (the lower one). (c) Flexible films of red and yellow p-PLDH in PVA films.

3.6. Thermal endurance

Solid fluorophores are important candidates in various nonlinear optical and optoelectronics devices. For these applications, thermo- and photo-stability of solidified fluorophores are critical concerns. We carried out the thermal endurance tests with p-PLDH and the bare PD as the comparison reference. Figure 7a shows the drop-casting PD and p-PLDH layer on a transparent PET substrate (1×1 cm^2), showing that the solid-state p-PLDH was much easier to form a uniform film coating than PD. The uneven distribution of PD could be presumably due to PD aggregation under a solvent-free environment. The emission of the PD layers faded away after 96 h of baking at 150ºC, and the remained fluorescence could be seen only at the edges (Figure 7a). In addition, the maximum emission wavelength of PD films exhibits a blue shift with increased heating time (Figure 7b), accompanied by an intensity decrease (at 640 nm) to 60% after 96 h of heating. The blue shift of the PD films can be attributed to the degradation of the conjugated polymer chain inside PD[63, 67]. On the other hand, the fluorescence of p-PLDH films remained extremely stable after 96 h of baking without any shift in the emission wavelength, suggesting the durable thermal stability of p-PLDH. The PL intensity ratios have increased until it exceeds 100% after 24 h of baking at 150ºC. The weaker PL before baking can be attributed to the interaction between absorbed water molecules and the PD chromophores within the LDH, which is possible according to theoretical and experimental investigations on some compounds with fluorescent chromophores[68-69]. This interaction may also be caused by the formation of localized electronic surface states[70], minimizing the optimum FL capabilities of PD. The thermal stability trend on

LDH composites associated with loss of water has also been reported in the LDH/(PVA-CdSe/ZnS) system[55] where the FL intensity increases over baking time.

We also incorporated p-PLDH in flexible polyvinyl alcohol (PVA) films (Figure 5c). The films of p-PLDH exhibit the homogenous fluorescence and bendable feature. We demonstrated that p-PLDH nanocomposites displayed enhanced thermal durability and excellent fluorescence stability, and can be doped into flexible substrates. LDH solidification can be promising for the future use of PD in solid-state optoelectronics.

4. CONCLUSIONS

We have successfully demonstrated PD solidification approaches with unquenched brightness and much improved photostability under harsh conditions and redispersiblility after solidification The synthesized nanomaterials are ideal for *in vitro*/*in vivo* bioimaging applications with minimal cytotoxicity as that of PDs. Moreover, the superior thermal durability of PLDH is noteworthy for potential applications in other areas such as light-emitting electronics. Physical mixing of method provides the extremely simple, time- and energy-effective process (10-min blending) with comparable performance to other synthetic methods designed in this study. The e robust PL performance in p-PLDH is due to the LDH sandwich assemblies and PD deshaping. The facile, one-pot combination of LDH with various fluorescent PDs (from blue to near-infrared) will create new avenues of robust PD-LDH hybrids in optical devices and bio-related technologies.

ASSOCIATED CONTENT

Supporting Information available: Photoluminescent spectra, XRD data, SEM images, Size distribution analysis, Optical measurement data, Time resolved fluorescent decay experiments

AUTHOR INFORMATION

Corresponding Authors

* yhchan@mail.nsysu.edu.tw (Y.-H. Chan), chunhu.chen@nsysu.edu.tw (C.-H. Chen)

Author Contributions

The manuscript was written through contributions of all authors. All authors have given approval to the final version of the manuscript.

ACKNOWLEDGMENT

We thank the funding support from Ministry of Science and Technology, Taiwan under Grant No. MOST 105-2113-M-110-003.

REFERENCES

1. Michalet, X.; Pinaud, F. F.; Bentolila, L. A.; Tsay, J. M.; Doose, S.; Li, J. J.; Sundaresan, G.; Wu, A. M.; Gambhir, S. S.; Weiss, S., Quantum Dots for Live Cells, in Vivo Imaging, and Diagnostics. *Science* **2005,** *307*, 538-544.

2. Karakoti, A. S.; Shukla, R.; Shanker, R.; Singh, S., Surface functionalization of quantum dots for biological applications. *Adv. Colloid Interface Sci.* **2015,** *215* (Supplement C), 28-45.

3. Yuan, L.; Lin, W.; Zheng, K.; Zhu, S., FRET-Based Small-Molecule Fluorescent Probes: Rational Design and Bioimaging Applications. *Acc. Chem. Res.* **2013,** *46* (7), 1462-1473.

4. Wei, Y.; Cheng, D.; Ren, T.; Li, Y.; Zeng, Z.; Yuan, L., Design of NIR Chromenylium-Cyanine Fluorophore Library for "Switch-ON" and Ratiometric Detection of Bio-Active Species In Vivo. *Anal. Chem.* **2016,** *88* (3), 1842-1849.

5. Jiang, Z. C.; Lin, T. N.; Lin, H. T.; Talite, M. J.; Tzeng, T. T.; Hsu, C. L.; Chiu, K. P.; Lin, C. A. J.; Shen, J. L.; Yuan, C. T., A Facile and Low-Cost Method to Enhance the Internal Quantum Yield and External Light-Extraction Efficiency for Flexible Light-Emitting Carbon-Dot Films. *Sci. Rep.* **2016,** *6*, 19991.

6. Zhang, X.; Shamirian, A.; Jawaid, A. M.; Tyrakowski, C. M.; Page, L. E.; Das, A.; Chen, O.; Isovic, A.; Hassan, A.; Snee, P. T., Monolayer Silane-Coated, Water-Soluble Quantum Dots. *Small* **2015,** *11* (45), 6091-6096.

7. Wang, F.; Xie, Z.; Zhang, H.; Liu, C.-y.; Zhang, Y.-g., Highly Luminescent Organosilane-Functionalized Carbon Dots. *Adv. Func. Mater.* **2011,** *21* (6), 1027-1031.

8. Lee, J. H.; Jung, D.-Y.; Kim, E.; Ahn, T. K., Fluorescein dye intercalated layered double hydroxides for chemically stabilized photoluminescent indicators on inorganic surfaces. *Dalton Trans.* **2014,** *43* (22), 8543-8548.

9. Cho, S.; Jung, S.; Jeong, S.; Bang, J.; Park, J.; Park, Y.; Kim, S., Strategy for Synthesizing Quantum Dot-Layered Double Hydroxide Nanocomposites and Their Enhanced Photoluminescence and Photostability. *Langmuir* **2013,** *29* (1), 441-447.

10. Wu, C.; Peng, H.; Jiang, Y.; McNeill, J., Energy Transfer Mediated Fluorescence from Blended Conjugated Polymer Nanoparticles. *J. Phys. Chem. B* **2006,** *110* (29), 14148-14154.

11. Chan, Y.-H.; Wu, C.; Ye, F.; Jin, Y.; Smith, P. B.; Chiu, D. T., Development of Ultrabright Semiconducting Polymer Dots for Ratiometric pH Sensing. *Anal. Chem.* **2011,** *83* (4), 1448-1455.

12. Wu, P.-J.; Kuo, S.-Y.; Huang, Y.-C.; Chen, C.-P.; Chan, Y.-H., Polydiacetylene-Enclosed Near-Infrared Fluorescent Semiconducting Polymer Dots for Bioimaging and Sensing. *Anal. Chem.* **2014,** *86* (10), 4831-4839.

13. Xiong, L.; Cao, F.; Cao, X.; Guo, Y.; Zhang, Y.; Cai, X., Long-Term-Stable Near-Infrared Polymer Dots with Ultrasmall Size and Narrow-Band Emission for Imaging Tumor Vasculature in Vivo. *Bioconjugate Chem.* **2015,** *26* (5), 817-821.

14. Ke, C.-S.; Fang, C.-C.; Yan, J.-Y.; Tseng, P.-J.; Pyle, J. R.; Chen, C.-P.; Lin, S.-Y.; Chen, J.; Zhang, X.; Chan, Y.-H., Molecular Engineering and Design of Semiconducting Polymer Dots with Narrow-Band, Near-Infrared Emission for in Vivo Biological Imaging. *ACS Nano* **2017,** *11* (3), 3166-3177.

15. Pecher, J.; Mecking, S., Nanoparticles of Conjugated Polymers. *Chem. Rev.* **2010,** *110* (10), 6260-6279.

16. Wu, C.; Chiu, D. T., Highly Fluorescent Semiconducting Polymer Dots for Biology and Medicine. *Angaw. Chem. Int. Ed. Engl.* **2013,** *52* (11), 3086-3109.

17. Howes, P.; Green, M., Colloidal and optical stability of PEG-capped and phospholipid-encapsulated semiconducting polymer nanospheres in different aqueous media. *Photochem. Photobiol.Sci.* **2010,** *9* (8), 1159-1166.

18. Wu, C.; Jin, Y.; Schneider, T.; Burnham, D. R.; Smith, P. B.; Chiu, D. T., Ultrabright and Bioorthogonal Labeling of Cellular Targets Using Semiconducting Polymer Dots and Click Chemistry. *Angewandte Chemie (International ed. in English)* **2010,** *49* (49), 9436-9440.

19. Yu, J.; Wu, C.; Zhang, X.; Ye, F.; Gallina, M. E.; Rong, Y.; Wu, I. C.; Sun, W.; Chan, Y.-H.; Chiu, D. T., Stable Functionalization of Small Semiconducting Polymer Dots via Covalent Cross-Linking and Their Application for Specific Cellular Imaging. *Adv. Mater.* **2012,** *24* (26), 3498-3504.

20. Ye, F.; Wu, C.; Sun, W.; Yu, J.; Zhang, X.; Rong, Y.; Zhang, Y.; Wu, I. C.; Chan, Y.-H.; Chiu, D. T., Semiconducting polymer dots with monofunctional groups. *Chem. Commun.* **2014,** *50* (42), 5604-5607.

21. Lyu, Y.; Zhen, X.; Miao, Y.; Pu, K., Reaction-Based Semiconducting Polymer Nanoprobes for Photoacoustic Imaging of Protein Sulfenic Acids. *ACS Nano* **2017,** *11* (1), 358-367.

22. Jiang, Y.; Upputuri, P. K.; Xie, C.; Lyu, Y.; Zhang, L.; Xiong, Q.; Pramanik, M.; Pu, K., Broadband Absorbing Semiconducting Polymer Nanoparticles for Photoacoustic Imaging in Second Near-Infrared Window. *Nano Lett.* **2017,** *17* (8), 4964-4969.

23. Xie, C.; Upputuri, P. K.; Zhen, X.; Pramanik, M.; Pu, K., Self-quenched semiconducting polymer nanoparticles for amplified in vivo photoacoustic imaging. *Biomaterials* **2017,** *119* (Supplement C), 1-8.

24. Lyu, Y.; Pu, K., Recent Advances of Activatable Molecular Probes Based on Semiconducting Polymer Nanoparticles in Sensing and Imaging. *Adv. Sci.* **2017,** *4* (6), 1600481-n/a.

25. Pu, K.; Chattopadhyay, N.; Rao, J., Recent advances of semiconducting polymer nanoparticles in in vivo molecular imaging. *J. Control. Release* **2016,** *240* (Supplement C), 312-322.

26. Sun, W.; Ye, F.; Gallina, M. E.; Yu, J.; Wu, C.; Chiu, D. T., Lyophilization of Semiconducting Polymer Dot Bioconjugates. *Anal. Chem.* **2013,** *85* (9), 4316-4320.

27. Carrado, K. A.; Kostapapas, A.; Suib, S. L., Layered double hydroxides (LDHs). *Solid State Ion.* **1988,** *26* (2), 77-86.

28. Wang, Q.; O'Hare, D., Recent Advances in the Synthesis and Application of Layered Double Hydroxide (LDH) Nanosheets. *Chem. Rev.* **2012,** *112* (7), 4124-4155.

29. Musumeci, A. W.; Mortimer, G. M.; Butler, M. K.; Xu, Z. P.; Minchin, R. F.; Martin, D. J., Fluorescent layered double hydroxide nanoparticles for biological studies. *Appl. Clay Sci.* **2010,** *48* (1), 271-279.

30. Tian, R.; Yan, D.; Wei, M., Layered Double Hydroxide Materials: Assembly and Photofunctionality. In *Photofunctional Layered Materials*, Yan, D.; Wei, M., Eds. Springer International Publishing: Cham, 2015; pp 1-68.

31. Song, L.; Shi, W.; Lu, C., Confinement Effect in Layered Double Hydroxide Nanoreactor: Improved Optical Sensing Selectivity. *Anal. Chem.* **2016,** *88* (16), 8188-8193.

32. Wei, P.-R.; Cheng, S.-H.; Liao, W.-N.; Kao, K.-C.; Weng, C.-F.; Lee, C.-H., Synthesis of chitosan-coated near-infrared layered double hydroxide nanoparticles for in vivo optical imaging. *J. Mater. Chem.* **2012,** *22* (12), 5503-5513.

33. Hibino, T., Delamination of Layered Double Hydroxides Containing Amino Acids. *Chem. Mater.* **2004,** *16* (25), 5482-5488.

34. Cho, S.; Kwag, J.; Jeong, S.; Baek, Y.; Kim, S., Highly Fluorescent and Stable Quantum Dot-Polymer-Layered Double Hydroxide Composites. *Chem. Mater.* **2013,** *25* (7), 1071-1077.

35. Li, Z.; Zhou, Y.; Yan, D.; Wei, M., Electrochemiluminescence resonance energy transfer (ERET) towards trinitrotoluene sensor based on layer-by-layer assembly of luminol-layered double hydroxides and CdTe quantum dots. *J. Mater. Chem. C* **2017,** *5* (14), 3473-3479.

36. Tian, R.; Zhang, S.; Li, M.; Zhou, Y.; Lu, B.; Yan, D.; Wei, M.; Evans, D. G.; Duan, X., Localization of Au Nanoclusters on Layered Double Hydroxides Nanosheets: Confinement-Induced Emission Enhancement and Temperature-Responsive Luminescence. *Adv. Func. Mater.* **2015,** *25* (31), 5006-5015.

37. Gao, R.; Zhao, M.; Guan, Y.; Fang, X.; Li, X.; Yan, D., Ordered and flexible lanthanide complex thin films showing up-conversion and color-tunable luminescence. *J. Mater. Chem. C* **2014,** *2* (45), 9579-9586.

38. Gao, R.; Yan, D., Layered host-guest long-afterglow ultrathin nanosheets: high-efficiency phosphorescence energy transfer at 2D confined interface. *Chem. Sci.* **2017,** *8* (1), 590-599.

39. Dong, S.; Liu, F.; Lu, C., Organo-Modified Hydrotalcite-Quantum Dot Nanocomposites as a Novel Chemiluminescence Resonance Energy Transfer Probe. *Anal. Chem.* **2013,** *85* (6), 3363-3368.

40. Song, L.; Shi, J.; Lu, J.; Lu, C., Structure observation of graphene quantum dots by single-layered formation in layered confinement space. *Chem. Sci.* **2015,** *6* (8), 4846-4850.

41. Shi, W.; He, S.; Wei, M.; Evans, D. G.; Duan, X., Optical pH Sensor with Rapid Response Based on a Fluorescein-Intercalated Layered Double Hydroxide. *Adv. Func. Mater.* **2010,** *20* (22), 3856-3863.

42. Liu, Z.-h.; Ooi, K.; Kanoh, H.; Tang, W.; Yang, X.; Tomida, T., Synthesis of Thermally Stable Silica-Pillared Layered Manganese Oxide by an Intercalation/Solvothermal Reaction. *Chem. Mater.* **2001,** *13* (2), 473-478.

43. Iyi, N.; Matsumoto, T.; Kaneko, Y.; Kitamura, K., Deintercalation of Carbonate Ions from a Hydrotalcite-Like Compound: Enhanced Decarbonation Using Acid−Salt Mixed Solution. *Chem. Mater.* **2004,** *16* (15), 2926-2932.

44. Li, L.; Ma, R.; Ebina, Y.; Iyi, N.; Sasaki, T., Positively Charged Nanosheets Derived via Total Delamination of Layered Double Hydroxides. *Chem. Mater.* **2005,** *17* (17), 4386-4391.

45. Liu, Z.; Ma, R.; Osada, M.; Iyi, N.; Ebina, Y.; Takada, K.; Sasaki, T., Synthesis, Anion Exchange, and Delamination of Co−Al Layered Double Hydroxide: Assembly of the Exfoliated Nanosheet/Polyanion Composite Films and Magneto-Optical Studies. *J. Am. Chem. Soc.* **2006,** *128* (14), 4872-4880.

46. Ma, R.; Liu, Z.; Takada, K.; Iyi, N.; Bando, Y.; Sasaki, T., Synthesis and Exfoliation of Co2+−Fe3+ Layered Double Hydroxides: An Innovative Topochemical Approach. *J. Am. Chem. Soc.* **2007,** *129* (16), 5257-5263.

47. Ma, R.; Liu, Z.; Li, L.; Iyi, N.; Sasaki, T., Exfoliating layered double hydroxides in formamide: a method to obtain positively charged nanosheets. *J. Mater. Chem.* **2006,** *16* (39), 3809-3813.

48. Yu, J.; Liu, J.; Clearfield, A.; Sims, J. E.; Speiegle, M. T.; Suib, S. L.; Sun, L., Synthesis of Layered Double Hydroxide Single-Layer Nanosheets in Formamide. *Inorg. Chem.* **2016,** *55* (22), 12036-12041.

49. Chan, Y.-H.; Wu, P.-J., Semiconducting Polymer Nanoparticles as Fluorescent Probes for Biological Imaging and Sensing. *Part. Part. Syst. Char.* **2015,** *32* (1), 11-28.

50. Clafton, S. N.; Beattie, D. A.; Mierczynska-Vasilev, A.; Acres, R. G.; Morgan, A. C.; Kee, T. W., Chemical Defects in the Highly Fluorescent Conjugated Polymer Dots. *Langmuir* **2010,** *26* (23), 17785-17789.

51. Valente, J. S.; Hernandez-Cortez, J.; Cantu, M. S.; Ferrat, G.; López-Salinas, E., Calcined layered double hydroxides Mg–Me–Al (Me: Cu, Fe, Ni, Zn) as bifunctional catalysts. *Catal. Today* **2010,** *150* (3), 340-345.

52. Lu, M.; Shan, Z.; Andrea, K.; MacDonald, B.; Beale, S.; Curry, D. E.; Wang, L.; Wang, S.; Oakes, K. D.; Bennett, C.; Wu, W.; Zhang, X., Chemisorption Mechanism of DNA on Mg/Fe Layered Double Hydroxide Nanoparticles: Insights into Engineering Effective SiRNA Delivery Systems. *Langmuir* **2016,** *32* (11), 2659-2667.

53. Al-Kady, A. S.; Gaber, M.; Hussein, M. M.; Ebeid, E.-Z. M., Structural and fluorescence quenching characterization of hematite nanoparticles. *Spectrochim. Acta A* **2011,** *83* (1), 398-405.

54. Choy, J.-H.; Kwak, S.-Y.; Park, J.-S.; Jeong, Y.-J., Cellular uptake behavior of [[gamma]-32P] labeled ATP-LDH nanohybrids. *J. Mater. Chem.* **2001,** *11* (6), 1671-1674.

55. Liang, R.; Yan, D.; Tian, R.; Yu, X.; Shi, W.; Li, C.; Wei, M.; Evans, D. G.; Duan, X., Quantum Dots-Based Flexible Films and Their Application as the Phosphor in White Light-Emitting Diodes. *Chem. Mater.* **2014,** *26* (8), 2595-2600.

56. Liu, J.; Chen, G.; Yang, J., Preparation and characterization of poly(vinyl chloride)/layered double hydroxide nanocomposites with enhanced thermal stability. *Polymer* **2008,** *49* (18), 3923-3927.

57. Zhou, L.; Geng, J.; Wang, G.; Liu, J.; Liu, B., A water-soluble conjugated polymer brush with multihydroxy dendritic side chains. *Polym. Chem.* **2013,** *4* (20), 5243-5251.

58. Keita, H.; Guzelturk, B.; Pennakalathil, J.; Erdem, T.; Demir, H. V.; Tuncel, D., Construction of multi-layered white emitting organic nanoparticles by clicking polymers. *J. Mater. Chem. C* **2015,** *3* (39), 10277-10284.

59. Singh, A.; Bezuidenhout, M.; Walsh, N.; Beirne, J.; Felletti, R.; Wang, S.; Fitzgerald, K. T.; Gallagher, W. M.; Kiely, P.; Redmond, G., Functionalization of emissive conjugated polymer nanoparticles by coprecipitation: consequences for particle photophysics and colloidal properties. *Nanotechnology* **2016,** *27* (30), 305603.

60. Zhao, M.-Q.; Zhang, Q.; Huang, J.-Q.; Tian, G.-L.; Nie, J.-Q.; Peng, H.-J.; Wei, F., Unstacked double-layer templated graphene for high-rate lithium–sulphur batteries. **2014,** *5*, 3410.

61. Gu, Z.; Atherton, J. J.; Xu, Z. P., Hierarchical layered double hydroxide nanocomposites: structure, synthesis and applications. *Chem. Commun.* **2015,** *51* (15), 3024-3036.

62. Li, L.; Feng, Y.; Li, Y.; Zhao, W.; Shi, J., Fe3O4 Core/Layered Double Hydroxide Shell Nanocomposite: Versatile Magnetic Matrix for Anionic Functional Materials. *Angaw. Chem. Int. Ed.* **2009,** *48* (32), 5888-5892.

63. Rong, Y.; Wu, C.; Yu, J.; Zhang, X.; Ye, F.; Zeigler, M.; Gallina, M. E.; Wu, I. C.; Zhang, Y.; Chan, Y.-H.; Sun, W.; Uvdal, K.; Chiu, D. T., Multicolor Fluorescent Semiconducting Polymer Dots with Narrow Emissions and High Brightness. *ACS Nano* **2013,** *7* (1), 376-384.

64. Jin, Y.; Ye, F.; Wu, C.; Chan, Y.-H.; Chiu, D. T., Generation of functionalized and robust semiconducting polymer dots with polyelectrolytes. *Chem. Commun.* **2012,** *48* (26), 3161-3163.

65. Dulbecco, R.; Vogt, M., PLAQUE FORMATION AND ISOLATION OF PURE LINES WITH POLIOMYELITIS VIRUSES. *J. Exp. Med.* **1954,** *99* (2), 167-182.

66. Chen, D.; Li, Q.; Meng, Z.; Guo, L.; Tang, Y.; Liu, Z.; Yin, S.; Qin, W.; Yuan, Z.; Zhang, X.; Wu, C., Bright Polymer Dots Tracking Stem Cell Engraftment and Migration to Injured Mouse Liver. *Theranostics* **2017,** *7* (7), 1820-1834.

67. Ljungqvist, N.; Hjertberg, T., Oxidative Degradation of Poly(3-octylthiophene). *Macromolecules* **1995,** *28* (18), 5993-5999.

68. Dobretsov, G. E.; Syrejschikova, T. I.; Smolina, N. V., On mechanisms of fluorescence quenching by water. *Biophysics* **2014,** *59* (2), 183-188.

69. Fletcher, K.; Bunz, U. H. F.; Dreuw, A., Fluorescence Quenching of Benzaldehyde in Water by Hydrogen Atom Abstraction. *ChemPhysChem* **2016,** *17* (17), 2650-2653.

70. Tetsuka, H.; Ebina, T.; Mizukami, F., Highly Luminescent Flexible Quantum Dot–Clay Films. *Adv. Mater.* **2008,** *20* (16), 3039-3043.

TABLE OF CONTENTS